

# Direct-Product Volumetric Parameterization of Handlebodies via Harmonic Fields

Jiazhi Xia  
 School of Computer Engineering  
 Nanyang Technological University  
 Singapore  
 Email: xiaj0002@ntu.edu.sg

Ying He  
 School of Computer Engineering  
 Nanyang Technological University  
 Singapore  
 Email: yhe@ntu.edu.sg

Xiaotian Yin  
 Department of Computer Science  
 Stony Brook University  
 Stony Brook, USA  
 Email: xyin@cs.sunysb.edu

Shuchu Han  
 School of Computer Engineering  
 Nanyang Technological University  
 Singapore  
 Email: schan@ntu.edu.sg

Xianfeng Gu  
 Department of Computer Science  
 Stony Brook University  
 Stony Brook, USA  
 Email: gu@cs.sunysb.edu

**Abstract**—Volumetric parameterization plays an important role for geometric modeling. Due to the complicated topological nature of volumes, it is much more challenging than the surface case. This work focuses on the parameterization of volumes with a boundary surface embedded in 3D space. The intuition is to decompose the volume as the direct product of a two dimensional surface and a one dimensional curve. We first partition the boundary surface into ceiling, floor and walls. Then we compute the harmonic field in the volume with a Dirichlet boundary condition. By tracing the integral curve along the gradient of the harmonic function, we can parameterize the volume to the parametric domain. The method is guaranteed to produce bijection for handlebodies with complex topology, including topological balls as a degenerate case. Furthermore, the parameterization is regular everywhere. We apply the proposed parameterization method to construct hexahedral mesh.

**Keywords**—Solid modeling, volume parameterization, hexahedral mesh, polycube, harmonic fields, handlebody, direct-product.

## I. INTRODUCTION

Most real-world shapes are volumetric. The need for volumetric parameterization is ubiquitous in various research fields. In medical imaging, for example, the registration between two 3D image data sets can be reduced to building a map between their underlying parameter domains. In finite element simulations, hexahedral meshes are a highly desired representation for volumes, while such a mesh can be easily built out of the parameterization using certain canonical domains.

Unlike the widely studied surface parameterization, volumetric parameterization has not drawn too much attention, this is mainly because of the intrinsic difference between surface and volume. For example, it is well-known that a harmonic map between a topological disk and a planar convex domain is diffeomorphic, if the boundary map is a homeomorphism. This result plays an important role in surface parameterization. Unfortunately, such an approach is not applicable for volumes, i.e., volumetric harmonic

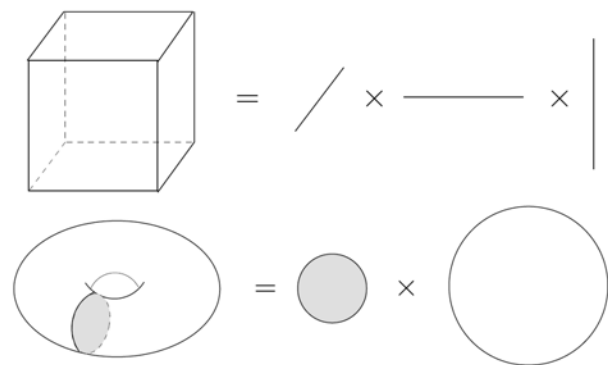


**Figure 1:** Handlebodies can be viewed as direct product of shapes in lower dimension. (a) Solid cube is the direct product of three line segments. (b) Solid torus is the direct product of a disk and a circle.

map does not guarantee to be bijective even though the parametric domain is convex. Therefore, it is technically challenging to generalize the surface parameterization to volume case.

In this work we focus on the parameterization of 3-dimensional handlebodies that can be decomposed into the direct product of 2-dimensional surface and a 1-dimensional curve. These models are very common in engineering fields, thus, the parameterization of such models is highly desirable. Note that many canonical domains have extremely simple structures. Some of them are just direct product of shapes from lower dimensions. Figure 1 shows examples including a solid cube, which is the direct product of three 1-dimensional line segments, and a solid torus, which is the direct product of a 2-dimensional disk and a 1-dimensional circle. The reason we prefer direct product domains is two-folded. Firstly, there is no singularity in a direct product domain, thus the parameterization would not degenerate at any point of the volume. Secondly, such structures will make many tasks easier, such as volumetric remeshing, volumetric

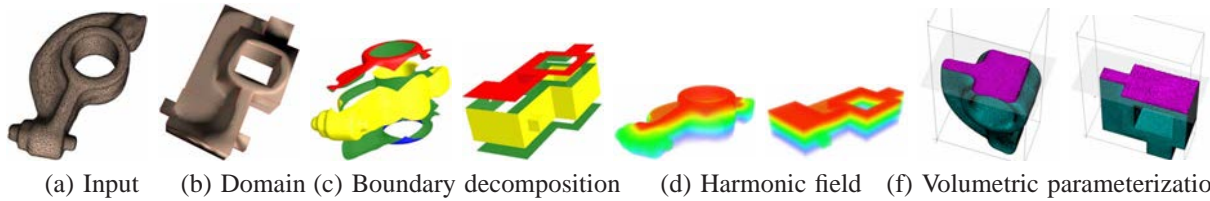


**Figure 2:** Direct product volumetric parameterization. The input is a tetrahedral mesh representing a 3D handlebody. We parameterize the boundary mesh to a polycube which also serves the parametric domain of the volume parameterization. Then we decompose the boundary mesh into ceiling (red), floor (blue) and walls (yellow). The ceiling and floors are topological annulus, the walls contain two topological cylinders. Next, we compute volumetric harmonic functions with the Dirichlet boundary conditions. Finally, the harmonic fields induce a homeomorphism between the handlebody and the polycube domain. The cut view illustrate the volumetric parameterization.

registration, physical simulation and so on.

Given a 3D handlebody  $M$ , we first construct a parametric domain  $P$ . To facilitate the hexahedral remeshing, we choose polycube due to its regular structure. Then, we compute a bijective map between the boundary surfaces  $\partial M$  and  $\partial P$ . Next, we partition  $\partial P$  into ceiling, floor and walls. The bijective polycube map induces the partition of  $\partial M$ . We compute the volumetric harmonic map with a Dirichlet boundary condition, i.e., the ceiling points are with boundary value 1, and floor points with boundary value 0. Finally, we construct a map between  $M$  and  $P$  by tracing the gradient field of harmonic functions. Figure 2 shows the parameterization of the genus-1 Rockerarm model to a polycube domain.

The proposed method has the following features:

- The algorithm is able to parameterize volumes with complex topology. It can also be downgraded and applied to volumes with trivial topology (i.e. topological balls).
- The parametric domain is simple and easy to construct. Loosely speaking, it is the direct product of a surface patch and a line segment. The resulted map between the original volume and the parameter domain is bijective, and there is no singularity. To our knowledge, our method is the first work that can guarantee the bijectivity of the parameterization for volumes with non-trivial topology.
- At any point in the volume, the  $w$  iso-parametric lines (which follow the gradient of the harmonic field) are orthogonal to  $u$  and  $v$  iso-parametric lines (which span the iso-surfaces of the harmonic field).

The rest of the paper is organized as follows. Section II briefly reviews the related work. Section III explains the necessary notations and background knowledge. The algorithm details are presented in Section IV, followed by some experimental results and comparisons in Section V. We conclude the paper and point out several future directions in Section VI.

## II. RELATED WORK

### A. Surface Parameterization

Surface parameterization has been extensively studied in the past decades. The survey papers by Sheffer et al [23] and Floater et al [8] are good reference for general interests. Many linear methods have been proposed for the conformal mapping. For example, DCP [6] and LSCM [14] are two of the earliest works that can handle multi-holed annuli. Both of them construct the mapping by solving certain linear systems with fixed or free boundary conditions. Slit map [35] is another linear method proposed to achieve regular boundaries of the annulus, where all the boundaries are mapped to parallel straight slits or concentric circles and arcs. Mullen et al [30] presented spectral conformal parameterization that finds the largest eigenvalue/eigenvector of a generalized eigenvalue problem involving sparse, symmetric matrices. This method does not have the common artifacts due to positional constraints on vertices.

Though computationally efficient, the above methods lack the flexible control on the boundaries. It turns out that finer control on the boundaries usually incurs much heavier computation. Discrete curvature flow uses curvature constraints to guide the metric deformation. Several non-linear computational methods have been proposed along this line, such as the circle pattern by Kharevych et al [13], the discrete Ricci flow by Jin et al [12] and the conformal equivalence by Springborn et al [24]. To alleviate the computational burden, Ben-Chen et al [1] proposed a linearized method with a trade-off that depends on applications. All these methods allow the users to design the boundary shape by prescribing the appropriate curvature on the boundary (as well as that inside).

### B. Volume Parameterization

Harmonic map plays an important role in surface parameterization. In [33], Wang et al generalized the surface harmonic map to volumes. They derived the formula of the the discrete harmonic map on tetrahedral meshes and then proposed a method to map genus-0 volumes to solid balls.

Li et al [15] [16] used the method of fundamental solution to build a mapping between volumes with the same topology. This method is essentially a simulation of electric fields over point clouds, and requires to place sufficient number of points (i.e. electric charges) off the boundary to enforce an approximated boundary condition. Li et al's method is able to parameterize the handlebodies, but it is computationally expensive to solve the harmonic map using fundamental solution method. Furthermore, the resulted map is not a bijection.

Martin et al [18] presented a method to parameterize volumes to the cylinder. By choosing a 1-dimensional skeleton inside the volume, they solved a harmonic map using the skeleton and the boundary surface as the boundary constraints. By tracing the gradient field of the harmonic function, they constructed a map between the volumes and the cylinder. Note that this method parameterizes only topological balls and can not process general handlebodies. Furthermore, the skeleton is the singularity of the constructed map.

Recently, Xia et al [34] showed that the Green's functions on star-shaped volume has a unique critical point and then developed a method to parameterize star shapes. The constructed map is guaranteed to be a diffeomorphism.

In contrast to the existing approaches, the proposed method is able to parameterize general handlebodies with a direct-product parameter domain without any singularity.

### C. Hexahedral Mesh Construction

Hexahedral meshes are widely used in computer-aided design and manufacturing due to its promising properties in the analysis stage [2], [5]. However, constructing high quality hexahedral mesh is a challenging problem [3].

The grid-based algorithms first fill the interior of the volume with a regular grid and then adaptively fit the boundary vertices [20], [21]. The generated meshes have nearly perfect elements in the interior, however, the quality near the boundary is usually poor.

Plastering [4] is a natural 3D extension of paving algorithms that have proven reliable for quadrilateral meshing on surfaces. Starting from the quadrilateral bounding meshes, fronts are determined and then advanced inward. This algorithm frequently has deficiencies when opposing fronts collide and can not resolve the unmeshed center voids due to being over-constrained by a pre-existing boundary mesh. The unconstrained plastering technique [25], [26] leverages the benefits of paving and plastering, without the over-constrained nature of plastering.

Whisker weaving algorithm [28], [29] also starts from a pre-defined boundary quad mesh. It first builds the combinatorial dual of a mesh based on the spatial twist continuum and then constructs the primal mesh and its embedding afterwards.

Embedded Voronoi graph contains the full symbolic information of the Voronoi diagram and the medial axis of the object, and a geometric approximation to the real geometry [7]. In [22], the algorithm uses the embedded Voronoi graph to decompose the volumes into simple sub-volumes that can be further meshed using conventional meshing methods. This method can handle arbitrary volume even if the medial axis is degenerate.

In our approach, we parameterize volumes to polycube domain. Note that the parametric domain is just the union of small cubes, thus, the parameterization induces a regular hexahedral meshing of the given volumes, i.e., every interior vertex is adjacent to exactly six edges. To our knowledge, none of the existing approaches can generate such regular hexahedral meshes.

### D. Polycube Map

Our algorithm is closely related to the polycube map which is used to compute the map between the boundary surfaces. The concept of polycube map was pioneered by Tarini et al [27]. Wang et al proposed an intrinsic method that guarantee to produce a one-to-one map between the polycube and 3D model [31]. Later, they developed a method that allows the user to specify the extraordinary points [32], and applied to the construction of manifold splines [9]. Lin et al presented an automatic algorithm to construct polycube maps for 3D models with simple geometry and topology [17]. Recently, He et al presented an algorithm to automatically construct polycube map [11]. By taking advantage of the divide-and-conquer strategy, their method can process large-scale models easily. However, their method is orientation dependent and usually leads to polycubes with large number of extraordinary points. To our knowledge, all these approaches focus on surface polycube maps, while our work starts from such a surface polycube map and then extends to the bounded volumes.

## III. THEORETICAL BACKGROUND

In this section we briefly introduce some necessary background knowledge that is underlying our algorithm, as well as the notations used in the paper.

### A. Handlebodies

In general, an  $n$ -hole ( $n \geq 1$ ) handlebody is a 3-manifold whose boundary is a surface that can be continuously deformed to some unknotted  $n$ -hole torus without tearing or self intersection. For such a volume  $H$ , its boundary surface  $\partial H$  can be covered by a set of charts,

$$\partial H = B_0 \cup B_1 \cup \bigcup_{i=0}^n D_i$$

where  $B_0$  and  $B_1$  are called *bases*, or to be specific,  $B_0$  is the *floor* and  $B_1$  the *ceiling* respectively. They are two disjoint  $n$ -hole annuli,  $B_0 \cap B_1 = \emptyset$ . Each  $D_i (i \in [0..n])$  is

called a *wall*, which is a topological cylinder with both ends open. All the walls are pairwise disjoint,  $D_i \cap D_j = \emptyset (i \neq j)$ . A base  $B_k (k \in \{0, 1\})$  and a wall  $D_l (l \in [0..n])$  intersect at a 1-dimensional simple loop,  $\zeta_{kl} = B_k \cap D_l$ . Figure 3 shows the Figure Eight model which is a 2-hole handlebody.

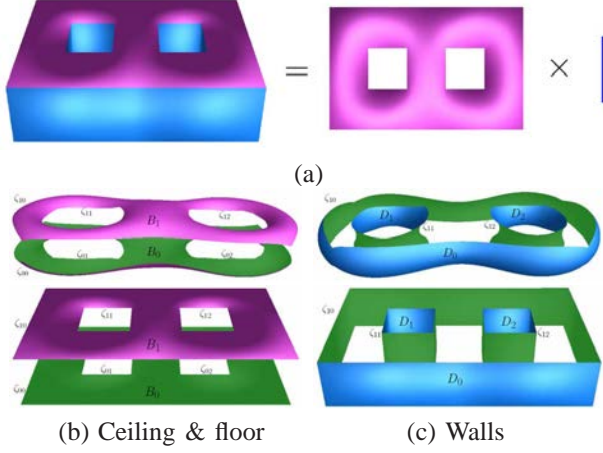


**Figure 3:** Direct product of Figure Eight model. The parametric domain (a genus-2 polycube) is the direct product of 2-hole disk and line segment, see (a). Both the volume and the polycube domain can be decomposed into ceiling, floor and walls, see (b)-(c).

As a special case, volumes without any handle (i.e. topological solid balls) can be considered as degenerate handle bodies with  $n = 0$ . The boundary surface for such bodies can also be partitioned into bases and walls, where each base is a topological disk and there is only one single wall.

### B. Volume Parameterization

For surfaces, parameterization is the process of computing a mapping between the original surface mesh in  $\mathbb{R}^3$  and a parametric domain that is usually a planar mesh in  $\mathbb{R}^2$ . This is equivalent to assigning a pair of real valued coordinates to every vertex in the mesh.

Parameterization for volumetric data can be defined in a similar fashion. Given a tetrahedral mesh  $M = (V, E, F, T)$  where  $V, E, F, T$  are the set of vertices, edges, triangles and tetrahedra respectively. Each vertex  $p_i \in V$  is assigned with a triple coordinates  $(u_i, v_i, w_i)$ . This is equivalent to compute three real valued parameter functions:

$$\{u, v, w\} : V \rightarrow \mathbb{R}$$

Note that although these functions are by definition restricted on vertices, it can be extended through out the whole tetrahedral mesh piecewisely. Namely, the function value for an arbitrary point in the volume is defined as the interpolation of the values on the four vertices of the tetrahedron. In this paper we use the same symbol to denote both the function restricted to vertices and that extended to the volume.

### C. Volumetric Harmonic Function

In general, a scalar function  $f$  is harmonic if it satisfies the Laplace's equation  $\Delta f = 0$  with Dirichlet boundary condition. This concept can be generalized to discrete tetrahedral mesh [33].

Given a tetrahedral mesh  $M$ , let  $f : V \rightarrow \mathbb{R}$  be a real valued function defined over the vertices, let  $f_i = f(p_i)$ ,  $p_i \in V$ .  $f$  is harmonic if and only if it satisfies the following discrete Laplace's equation:

$$\sum_{e_{ij} \in E} k_{ij}(f_j - f_i) = 0$$

where  $e_{ij}$  is an edge connecting vertex  $p_i$  to  $p_j$  and  $k_{ij}$  is a real valued weight assigned with  $e_{ij}$ . Following [33] [19], we define the weights as follows. Suppose edge  $e_{ij}$  is shared by  $m$  adjacent tetrahedra, it lies against  $m$  dihedral angles  $\{\theta_k\}$ ,  $k = 1, \dots, m$ . Then the edge weight for  $e_{ij}$  can be defined as  $k_{ij} = \frac{1}{12} \sum_{k=1}^m l_{ij} \cot \theta_k$ , where  $l_{ij}$  is the length of edge  $e_{ij}$ .

Same to that in the smooth setting, we can impose Dirichlet boundary conditions on the discrete volumetric harmonic function. Namely, we set the value of  $f$  fixed on certain vertices  $v_i \in V_c$ , where  $V_c$  is the set of vertices that serve as constrained vertices.

Once a harmonic function  $f$  is computed over a tetrahedral mesh, one can compute its gradient  $\nabla f$ , which is a vector field that is piecewise constant. An integral curve of the gradient vector field is a curve such that the tangent vector equals the gradient. Tracing such integral curves will lead to a volumetric parameterization.

## IV. DIRECT PRODUCT VOLUMETRIC PARAMETERIZATION

### A. Overview

In this section, we choose the polycube as the parametric domain due to the following reasons: first, polycube has a regular structure and can be used to construct all-hexahedral meshes; second, there are well-developed techniques to construct the polycube map that serves the map between the boundary surfaces; third, due to the geometric simplicity, it is usually easier to partition the boundary surface of polycube than that of the input model.

Since the goal is to parameterize the given volume  $M$  to the polycube  $P$ , we need to compute the parameter functions  $(u, v, w)_M$  and  $(u, v, w)_P$  for  $M$  and  $P$  respectively. Then we construct a function that maps  $(u, v)_M$  to  $(u, v)_P$ . Finally, the parameterization  $\phi : M \rightarrow P$  is induced by the map  $(u, v, w)_M \rightarrow (u, v, w)_P$ . This idea can be illustrated using the following commutative diagram:

$$\begin{array}{ccc}
M & \xrightarrow{\phi: M \rightarrow P} & P \\
\downarrow & & \downarrow \\
(u, v, w)_M & \xrightarrow{h: (u, v)_M \rightarrow (u, v)_P} & (u, v, w)_P
\end{array}$$

The proposed direct product volume parameterization contains the following steps:

- Input: A tetrahedral mesh  $M$  for a handle body and a polycube  $P$ .
- Output: A bijection  $\phi : M \rightarrow P$ .
  - 1) Partition the boundary surfaces  $\partial M$  and  $\partial P$  into bases  $B_i$  and walls  $D_j$  ;
  - 2) Compute harmonic functions  $f_M$  and  $f_P$  using the partition as Dirichlet boundary conditions;
  - 3) Trace the integral curves for every interior vertex.
  - 4) Trace the integral curves on the walls.

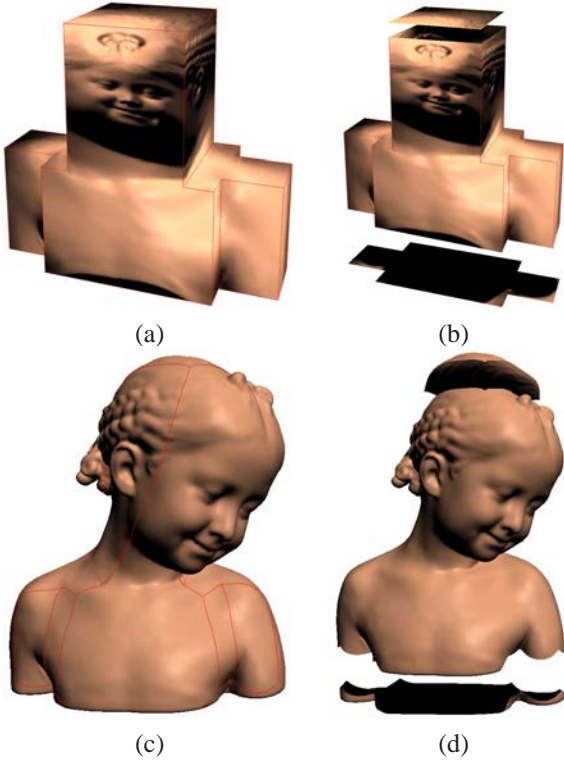


**Figure 4:** Partition the boundary surface into ceiling, floor and walls. We first construct the polycube map for the boundary surface. The top and bottom faces of the polycube serve the ceiling and floor and the remaining part is the wall. The polycube map induces the surface partition on the 3D model.

### B. Computing the harmonic fields

Given a tetrahedral mesh  $M$  and the user-constructed polycube domain  $P$ , we first construct the polycube map between the boundary surfaces  $\partial M$  and  $\partial P$  using the divide-and-conquer approach by [11]. We design the polycube

manually to reduce its complexity which facilitates the boundary decomposition. Then, we partition the boundary surfaces into bases (ceiling and floor) and walls. Note that the polycube domain has simpler structure than the original surface. Thus, it is much easier to partition the polycube boundary surface than the original model. To do this, the user just simply choose the desired polycube faces by several mouse clicks. By taking advantage of the bijectivity of the polycube map, the partition of  $\partial P$  naturally induces a partition of  $\partial M$ . Let  $B_i^M$  and  $B_i^P$  denote the bases for  $\partial M$  and  $\partial P$  respectively. Similar,  $D_j^M$  and  $D_j^P$  denote the walls. Figure 4 and 8 show the partition of the genus-0 Bimba and genus-2 Cup via the polycube maps.

With the ceiling/floor/wall partition, we are ready to compute the harmonic fields for both  $M$  and  $P$ . Specifically, we solve two harmonic functions  $f_M : M \rightarrow \mathbb{R}$  and  $f_P : P \rightarrow \mathbb{R}$ , such that

$$\begin{aligned}
\Delta f(p) &= 0, \quad \forall p \notin B_0 \cup B_1 \\
f(p) &= 0, \quad \forall p \in B_0 \\
f(p) &= 1, \quad \forall p \in B_1.
\end{aligned}$$

Figure 5 show the computed harmonic fields in  $M$  and  $P$  of the genus-0 Bimba model.

### C. Tracing inside the volume

To trace the integral curve, we need to compute the gradient of  $f_M$  and  $f_P$ . Given an arbitrary scalar function  $g$ , the gradient  $\nabla g$  can be computed as follows [10]: suppose  $t_{ijkl}$  is a tetrahedron with vertices  $\{p_i, p_j, p_k, p_l\}$ , the face on the tetrahedron against vertex  $p_i$  is  $f_i$ ; similarly  $p_j, p_k$ , and  $p_l$  are against  $f_j, f_k$ , and  $f_l$ , respectively. We define  $\mathbf{s}_i$  to be the vector along the normal of  $f_i$  with length equal to 2 times the area of  $f_i$ , and so can  $\mathbf{s}_j, \mathbf{s}_k, \mathbf{s}_l$  be defined. Then, the gradient of  $g$  in  $t_{ijkl}$  is a constant vector field

$$\nabla g = g(p_i)\mathbf{s}_i + g(p_j)\mathbf{s}_j + g(p_k)\mathbf{s}_k + g(p_l)\mathbf{s}_l.$$

We then define the vertex gradient as the average of the gradient vectors in the neighboring tetrahedra.

The parameterization from the  $M$  to  $P$  is constructed as follows: given an interior point  $s \in M$ , we trace the integration curve  $\gamma$  of the gradient field  $\nabla f_M$ . The integration curve  $\gamma$  intersects the ceiling and floor at  $p \in B_1^M$  and  $q \in B_0^M$ .

Using the polycube map, we can define a floor map  $h : B_0^M \rightarrow B_0^P$  that maps each floor point  $q \in B_0^M$  to  $q' \in B_0^P$ .

Then we compute an integral curve  $\gamma'$  starting from  $q'$  and following  $\nabla f_P$ .  $\gamma'$  intersects the ceiling at  $p' \in B_1^P$ . Then we can find a unique point  $s' \in \gamma'$  such that  $f_P(s') = f_M(s)$ . The point  $s' \in P$  is the image of  $s$ , i.e.,  $\phi(s) = s'$ . By computing the images for every interior vertex in  $M$ , we build the parameterization between the interior of  $M$  and  $P$ .

Note that each integral curve starts from a point on the floor and then terminates at a point on the ceiling. Since

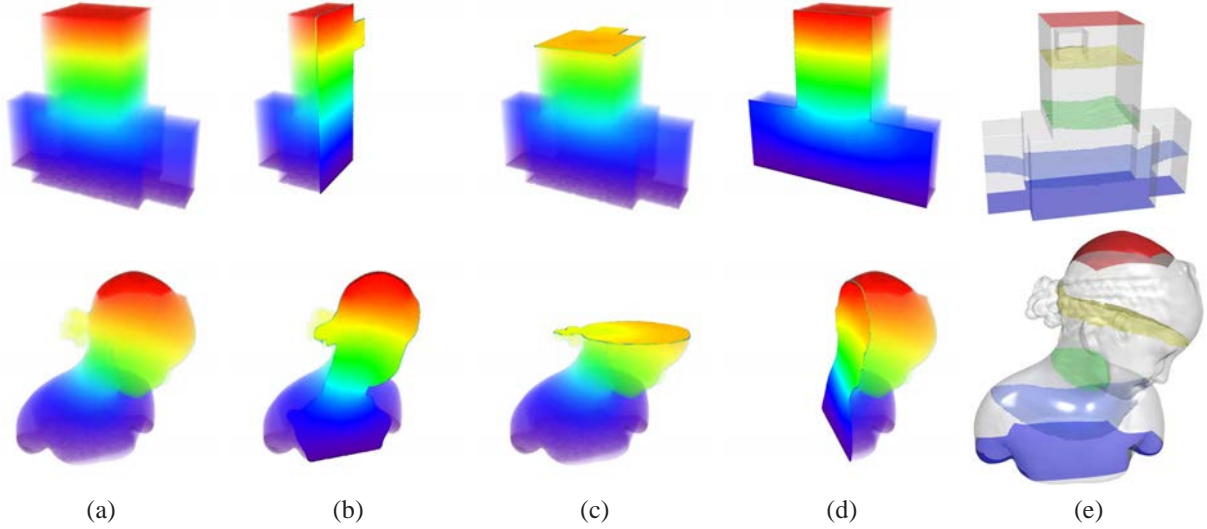


**Figure 5:** Computing the harmonic fields of the genus-0 Bimba model. We solve a volumetric harmonic map  $\Delta f = 0$  with boundary conditions  $f(B_0) = 0$  and  $f(B_1) = 1$ . The volume renderings (a)-(d) show the computed harmonic fields on the polycube and 3D model. (e) shows several iso-surfaces of harmonic fields.

the floor is a  $g$ -hole disc if  $\partial M$  is of genus- $g$ , we can map the  $g$ -hole disc to planar domain and then assign a parameter  $(u, v)$  for each integral curve, i.e., all points on the same integral curve share the same  $u$ , and  $v$  parameters, they only differ by  $w$ -parameter, which is determined by the arc-length parameterization. Figure 6 and 9 show tracing the integral curves inside the volumes.

#### D. Tracing on the walls

In the previous step, we construct the map for the interior vertices. Now, we want to build the map between walls. Tracing the integral curve on the walls can be viewed as the degenerate case of tracing inside the volumes. Restricting the volumetric harmonic function on the walls, we have the surface harmonic function denoted by  $g_D$ .

Given a triangle  $t_{ijk} = \{p_i, p_j, p_k\}$ , let  $e_i$ ,  $e_j$  and  $e_k$  denote the opposite edges. We define a rotation operator  $rot$  that rotates the edge 90 degree outwards the triangle. Then the gradient on the triangle  $t_{ijk}$  is given by

$$\nabla g_D = g_D(p_i)rot(e_i) + g_D(p_j)rot(e_j) + g_D(p_k)rot(e_k).$$

Starting from the vertices on the boundary of floor  $\partial B_0$ , we trace the integral curve following the gradient of  $g_D$ . The integral curves are perpendicular to the iso-curves of  $g_D$  and terminates on the boundary of ceiling  $\partial B_1$ . Figure 7 shows tracing the integral curves on the walls.

Note that the floor map  $h : B_0^M \rightarrow B_0^P$  is a bijection, as  $h$  is constructed by restricting the polycube map to the floor. An integral curve is given by a unique  $(u, v)$  parameter and the points on the same integral curve are differed by the  $w$  parameter. Thus, the floor map  $h$  maps an integral curve in  $M$  to a unique integral curve in  $P$ , which in turn maps a point in  $M$  to a unique point in  $P$ . So, by

tracing the integral curves for every floor point, we build the piecewise parameterization between  $M$  and  $P$ .

#### E. Properties

The proposed direct product volumetric parameterization is guaranteed to be bijective.

*Theorem:* The handlebody  $M$  and its parametric domain  $P$  are partitioned into ceiling, floor and walls,  $M = B_0^M \cup B_1^M \cup \bigcup_{i=0}^n D_i^M$ ,  $P = B_0^P \cup B_1^P \cup \bigcup_{i=0}^n D_i^P$ . Define harmonic function on  $M$ ,  $f_M : M \rightarrow \mathbb{R}$ ,  $\Delta f_M = 0$ , with Dirichlet boundary condition,  $f_M|_{B_0^M} = 0$  and  $f_M|_{B_1^M} = 1$ . The harmonic function on  $P$ ,  $f_P : P \rightarrow \mathbb{R}$ , is defined in a similar fashion. Define a floor map  $h : B_0^M \rightarrow B_0^P$  from the  $M$ 's floor to  $P$ 's. If  $h$  is a bijection, then the harmonic functions induced volumetric parameterization is also a bijection.

Proof:

First, we show that two integral curves can not intersect in  $M$  and  $P$ . Without loss of generality, let  $\gamma_1$  and  $\gamma_2$  be two integral curves inside  $M$ . Assume they intersect at one point  $p$ , then at  $p$ , the gradient of  $f_M$  vanishes.  $p$  is a critical point. If  $p$  is an interior point, because  $f_M$  is harmonic, the maximum and minimum must be on the boundaries. Therefore the Hessian matrix at  $p$  has negative eigenvalue values. Suppose  $f_M(p) = s$ , then according to Morse theory, the homotopy types of the level sets  $f^{-1}(s - \epsilon)$  and  $f^{-1}(s + \epsilon)$  will be different. At all the interior critical points, the Hessian matrices have negative eigenvalues, the homotopy type of the level sets will be changed. The changes of the homotopy type can be not canceled out. Therefore, the homotopy type of the bottom should be different from that of the ceiling. Contradiction. Therefore,  $\gamma_1$  and  $\gamma_2$  can not intersect at any interior point.

If  $\gamma_1$  and  $\gamma_2$  intersect at a point  $p$  on the ceiling. Then we can glue two copies of the same volume, along their ceilings. And reverse the gradient field of one volume. The union of the two gradient fields give us a harmonic function field. Then there is no interior critical point on the doubled volume.  $p$  becomes one interior critical point. Contradiction again. Therefore  $\gamma_1$  and  $\gamma_2$  have no intersection points anywhere.

Next, we show that the integral curves induce a bijection between  $M$  and  $P$ . Given  $v^M \in B_0^M$  a point on the floor of  $M$ , let  $v^P = h(v^M)$  be the image on the floor of  $P$ . Starting from  $v^M$  and  $v^P$ , we get two integral curves  $\gamma_M \in M$  and  $\gamma_P \in P$  following the gradient of  $f_M$  and  $f_P$  respectively.

Since the integral curves can not intersect inside the volume and on the ceiling, the arc-length parameterization induces a bijection between  $\gamma_M$  and  $\gamma_P$ . If the function  $h$  is a bijection, each floor vertex on  $M$  is uniquely mapped to a floor vertex on  $P$ , which in turn maps an integral curve in  $M$  uniquely to an integral curve in  $P$ . Thus, the induced parameterization is a bijection. QED.

Our method can also guarantee that at any point in the volume, the  $w$  parametric line is orthogonal to  $u$  and  $v$  parametric lines, which is a natural consequence of enforcing a conformal parameterization on the surface and a gradient field in the volume. The reason is as follows: we map each integral curve in  $M$  to a unique integral curve in  $P$ . Both integral curves follow the gradient vector field of the harmonic function, thus, are orthogonal to the iso-surfaces of the harmonic function. Note that the iso-surface induces the  $u$  and  $v$  parameters and the integral curve induces the  $w$  parameter, thus, the  $w$  iso-parametric line is perpendicular to  $u$ - and  $v$ - lines.

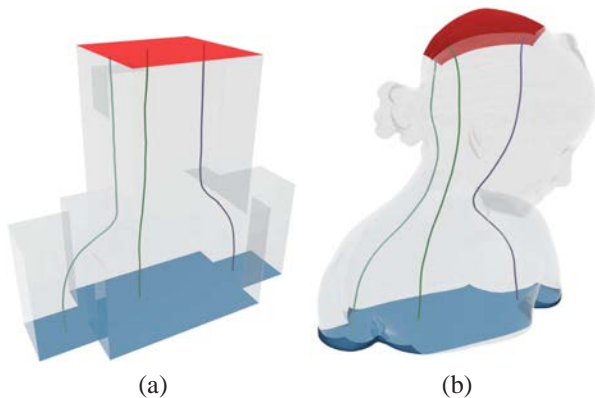


**Figure 6:** Tracing the integral curves in the volumes. The integral curves follow the gradient field of the harmonic function and is perpendicular to the floor and ceiling. Three pairs of integral curves are shown in  $M$  and  $P$ . The corresponding curves are drawn in the same color. Intuitively speaking, the position of the starting point on the floor induces the  $u$  and  $v$  parameters, and the integral curve induces the  $w$  parameter.

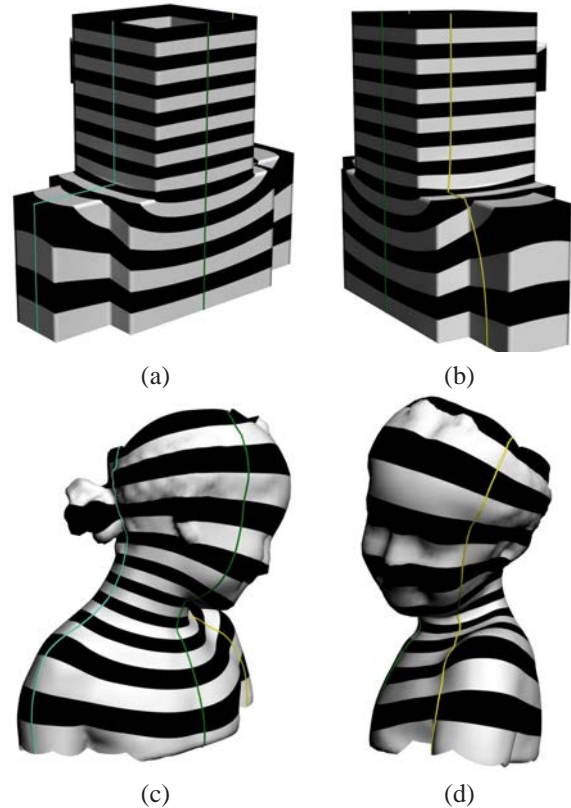


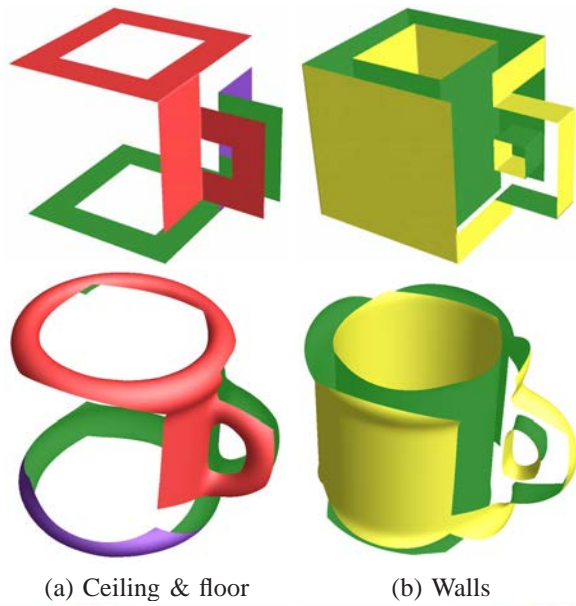
**Figure 7:** Tracing the integral curves on the walls. The texture mapping shows the iso-curves of the harmonic function restricted to the wall. The integral curve follows the harmonic function and is perpendicular to the boundary of the walls. Three pairs of integral curves are shown in  $M$  and  $P$ . The corresponding curves are drawn in the same color.

## V. EXPERIMENTAL RESULTS

We tested our algorithm on models with various topology, including, Bimba (genus-0), Rockerarm (genus-1), Cup (genus-2) and Eight (genus-2).

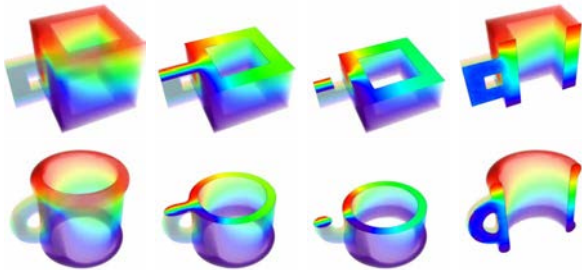
We computed the polycube map using the variant of divide-and-conquer method [11]. In [11], He et al's method can construct the polycube automatically by segmenting the shapes using horizontal planes and then approximate each part using voxelization-like approach. The resulted polycube is often complicated and has large number of corners that are extraordinary points of the polycube map. To reduce the number of singularities, we prefer to construct the polycube manually. The divide-and-conquer framework [11] can still apply to the manually constructed polycube.

Taking advantage of the polycube map, we developed a user-friendly interface that allows the users to easily select the polycube faces by simple mouse click. With the user-specified Dirichlet boundary condition, we solved the discrete harmonic function using finite element method. We used volume rendering to visualize the harmonic field

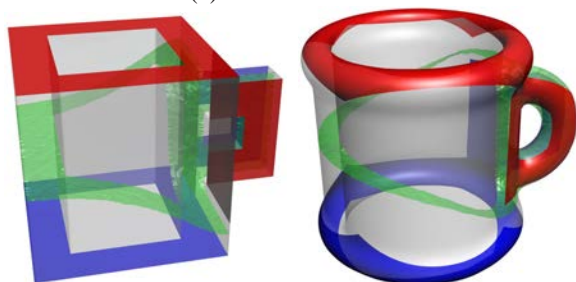


(a) Ceiling & floor

(b) Walls



(c) Harmonic fields



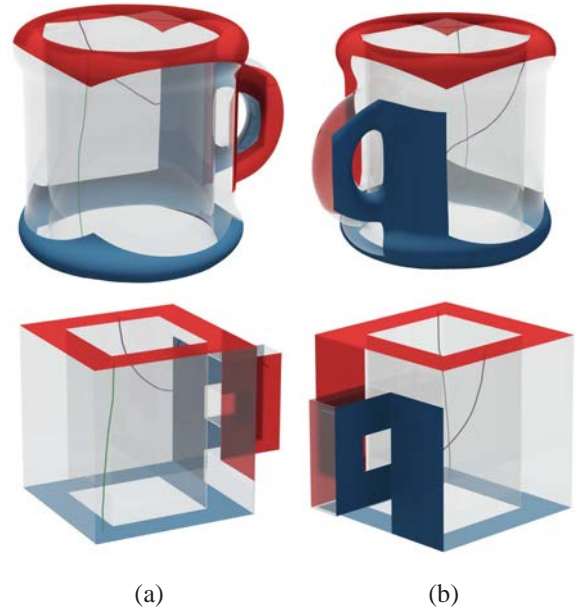
(d) Isosurface of harmonic fields

**Figure 8:** Direct product parameterization of the genus-2 Cup model. (a) and (b) show the ceiling, floor and wall decomposition. Each ceiling/floor is 2-hole disk and the wall contains three topological cylinders. (c) shows the volume rendering of the harmonic fields. (d) show the isosurface of the harmonic fields.

inside the volumes, as shown in Fig. 2(d), 5 and 8.

We demonstrated the proposed volumetric parameterization algorithm on hexahedral mesh generation. Note that the polycube domain has very natural hexahedral tessellation. The volumetric parameterization induces a map between the polycube and the given volume. Thus, it also induces a hexahedral tessellation in the volume dataset as shown in Fig. 10.

We compared our method with the existing approaches [33], [15], [18] and [34]. In [33], the volume



(a)

(b)

**Figure 9:** Tracing the integral curves in  $M$  and  $P$ . (a) and (b) show two different views of three integral curves. The ceiling and floor are drawn in red and blue respectively. The walls are rendered transparently. The corresponding curves are drawn in the same color.



**Figure 10:** Construction of the hexahedral mesh using direct-product volumetric parameterization.

**Table I: Comparison to the existing approaches.**

	Wang [33]	Li [15]	Martin [18]	Xia [34]	Ours
Topology	Topological balls	Arbitrary bounded volumes	Topological balls	Star-shaped volumes	Handlebody
Singularity	No	No	1d skeleton	center point	No
Bijectivity	No	No	Yes	Yes	Yes

boundary is first mapped to the unit sphere, the boundary mapping is a diffeomorphism. Then the boundary diffeomorphism is extended to the interior by solving a volumetric Dirichlet problem, using the boundary mapping as the boundary conditions. Wang et al used finite element method to solve the volumetric Dirichlet problem. In [15], Li et al used fundamental solution method, which doesn't require the tessellation of the volume to solve the exact same Dirichlet problem. In two dimensional case, Rado's theorem claims that if the target domain is convex, then harmonic maps are diffeomorphisms. Unfortunately, in volumetric case, even the target is convex and boundary mapping is diffeomorphic, the volumetric harmonic map may not be diffeomorphic. Therefore, neither Wang et al. method [33] nor Li et al method [15] can not guarantee the final mapping to be diffeomorphic. In [18], Martin et al first specified a 1-dimensional skeleton inside the volume and solve the volumetric harmonic map with Dirichlet boundary conditions of the skeleton and the boundary surface. The parameterization is constructed by tracing the gradient field of the harmonic function. Martin et al's method works only for topological balls where the homotopy type of the offset surface of the skeleton is the same as the boundary surface. Furthermore, the skeleton are the critical points of the harmonic map, thus, the resulted parameterization is singular on the skeleton. In [34], Xia et al. proved that the Green's function on star shaped volume has a unique critical point, i.e., the center of the star shape. As a result, the integration curves of the gradient of the Green's function do not intersect except at the center point. Then they developed a method to parameterize star-shaped volumes by tracing the integration curves of the gradient of the Green's functions. Xia et al's method is guaranteed to be a diffeomorphism. However, it only applies to star-shaped volumes.

Our method is different from the above approaches in three aspects: first, our method is guaranteed to be a bijection if the floor map is bijective; second, our method works for volumes with complex topology and geometry; third, our parameterization does not have any singularity, thus, is regular everywhere. Table I summarizes the properties of the existing volumetric parameterization algorithms and our method.

## VI. CONCLUSIONS AND FUTURE WORK

In this paper, we present a novel approach to parameterize volumes using harmonic fields. We first partition the boundary surface into ceiling, floor and walls. Then we compute the harmonic fields using the Dirichlet boundary conditions. Next, by tracing the gradient of the harmonic

function, we can parameterize the given volume to the parametric domain, such as a polycube. In contrast to the existing approaches, the proposed algorithm guarantees to produce a bijection without singularities. Furthermore, it is able to parameterize volumes of non-trivial topology and geometry.

The proposed algorithm has limitations. Firstly, the decomposition for the models with complicated topology/geometry may not be intuitive. For example, the two handles of the genus-2 Cup model is twisted. Thus, it requires the users to be very skilled and experienced to decompose the boundary mesh. Secondly, tracing the integral curves highly depends on the quality of the tetrahedral mesh. In the future, we will develop automatic algorithm to partition the boundary surface. We will also investigate robust and efficient algorithm to improve the tracing step.

## ACKNOWLEDGMENT

The work was partially supported by AcRF 69/07, NSF CCF-1081424, ONR N000140910228, CCF-0448399, and CCF-0830550. The models are courtesy of Aim@Shape Shape Repository. We would like to thank the anonymous reviewers for their careful reviews and constructive comments.

## REFERENCES

- [1] M. Ben-Chen, C. Gotsman, and G. Bunin. Conformal flattening by curvature prescription and metric scaling. *Computer Graphics Forum (Proc. Eurographics)*, 27(2), 2008.
- [2] S. E. Benzley, E. Perry, K. Merkle, and G. Clark, Brett Sjaardema. A comparison of all-hexahedral and all-tetrahedral finite element meshes for elastic and elastoplastic analysis. In *4th International Meshing Roundtable*, pages 179–191, 1995.
- [3] T. Blacker. Meeting the challenge for automated conformal hexahedral meshing. In *9th International Meshing Roundtable*, pages 11–20, 2000.
- [4] S. A. Canann. Plastering: A new approach to automated 3-d hexahedral mesh generation. 1992.
- [5] A. O. Cifuentes and A. Kalbag. A performance study of tetrahedral and hexahedral elements in 3-d finite element structural analysis. *Finite Elements in Analysis and Design*, 12(3-4):313–318, 1992.

- [6] M. Desbrun, M. Meyer, and P. Alliez. Intrinsic parameterizations of surface meshes. *Computer Graphics Forum*, 21:209–218, 2002.
- [7] M. Etzion and A. Rappoport. Computing voronoi skeletons of a 3-d polyhedron by space subdivision. *Computational Geometry: Theory and Applications*, 21(3):87–120, 2002.
- [8] M. S. Floater and K. Hormann. Surface parameterization: a tutorial and survey. In *Advances in Multiresolution for Geometric Modelling*, pages 157–186. Springer, 2005.
- [9] X. Gu, Y. He, and H. Qin. Manifold splines. *Graphical Models*, 68(3):237–254, 2006.
- [10] X. Gu, and S.-T. Yau. Computational conformal geometry. International Press, 2008.
- [11] Y. He, H. Wang, C.-W. Fu, and H. Qin. A divide-and-conquer approach for automatic polycube map construction. *Comput. Graph.*, 33(3):369–380, 2009.
- [12] M. Jin, J. Kim, F. Luo, and X. Gu. Discrete surface ricci flow. *TVCG*, 14(5):1030–1043, 2008.
- [13] L. Kharevych, B. Springborn, and P. Schröder. Discrete conformal mappings via circle patterns. *ACM Transactions on Graphics*, 25(2):412–438, 2006.
- [14] B. Lévy, S. Petitjean, N. Ray, and J. Maillot. Least squares conformal maps for automatic texture atlas generation. *ACM Transactions on Graphics*, 21(3):362–371, 2002.
- [15] X. Li, X. Guo, H. Wang, Y. He, X. Gu, and H. Qin. Harmonic volumetric mapping for solid modeling applications. In *Proceedings of ACM Symposium on Solid and Physical Modeling (SPM '07)*, pages 109–120, 2007.
- [16] X. Li, X. Guo, H. Wang, Y. He, X. Gu, and H. Qin. Meshless harmonic volumetric mapping using fundamental solution methods. *IEEE Trans. on Automation Science and Engineering*, 6(3):409–422, 2009.
- [17] J. Lin, X. Jin, Z. Fan, and C. C. L. Wang. Automatic polycube-maps. In *Proceedings of Geometric Modeling and Processing (GMP '08)*, pages 3–16, 2008.
- [18] T. Martin, E. Cohen, and M. Kirby. Volumetric parameterization and trivariate b-spline fitting using harmonic functions. In *Proceeding of Symposium on Solid and Physical Modeling*, pages 269–280, 2008.
- [19] M. Reuter, F.-E. Wolter, and N. Peinecke. Laplace-beltrami spectra as “shape-DNA” of surfaces and solids. *Computer Aided Design*, 38(4):342–366, 2006.
- [20] R. Schneiders. A grid-based algorithm for the generation of hexahedral element meshes. *Engineering with Computers*, 12(3-4):168–177, 1996.
- [21] R. Schneiders, R. Schindler, and F. a. Weiler. Octree-based generation of hexahedral element meshes. In *5th International Meshing Roundtable*, pages 205–215, 1996.
- [22] A. Sheffer, M. Etzion<sup>1</sup>, A. Rappoport, and M. Bercovier. Hexahedral mesh generation using the embedded voronoi graph. 15:248–262, 1999.
- [23] A. Sheffer, E. Praun, and K. Rose. Mesh parameterization methods and their applications. *Foundations and Trends<sup>®</sup> in Computer Graphics and Vision*, 2(2), 2006.
- [24] B. Springborn, P. Schröder, and U. Pinkall. Conformal equivalence of triangle meshes. *TOG*, 27(3).
- [25] M. L. Staten, R. A. Kerr, S. J. Owen, and T. D. Blacker. Unconstrained paving and plastering: Progress update. In *15th International Meshing Roundtable*, pages 469–486, 2006.
- [26] M. L. Staten, S. J. Owen, and T. D. Blacker. Unconstrained paving & plastering: A new idea for all hexahedral mesh generation. In *14th International Meshing Roundtable*, pages 399–416, 2005.
- [27] M. Tarini, K. Hormann, P. Cignoni, and C. Montani. Polycube-maps. *ACM Trans. Graph.*, 23(3):853–860, 2004.
- [28] T. J. Tautges, T. Blacker, and S. A. Mitchell. The whisker weaving algorithm: A connectivity-based method for constructing all-hexahedral finite element meshes. *International Journal for Numerical Methods in Engineering*, 39:3327–3349, 1996.
- [29] T. J. Tautges and S. A. a. Mitchell. Whisker weaving: Invalid connectivity resolution and primal construction algorithm. In *4th International Meshing Roundtable*, pages 115–127, 1995.
- [30] P. Mullen and Y. Tong and P. Alliez and M. Desbrun. Spectral Conformal Parameterization. In *Symposium of Geometry Processing*, 2008.
- [31] H. Wang, Y. He, X. Li, X. Gu, and H. Qin. Polycube splines. *Computer-Aided Design*, 40(6):721–733, 2008.
- [32] H. Wang, M. Jin, Y. He, X. Gu, and H. Qin. User-controllable polycube map for manifold spline construction. In *Proceedings of ACM Symposium on Solid and Physical Modeling (SPM '08)*, pages 397–404, 2008.
- [33] Y. Wang, X. Gu, P. M. Thompson, and S.-T. Yau. Volumetric harmonic map. *Communications in Information and Systems*, 3(3):191–202, 2004.
- [34] J. Xia, Y. He, S. Han, C.-W. Fu, F. Luo, and X. Gu. Parametrization of star-shaped volumes using Green’s functions. In *Proceedings of Geometric Modeling and Processing (GMP '10)*, to appear, 2010.
- [35] X. Yin, J. Dai, S.-T. Yau, and X. Gu. Slit map: Conformal parameterization for multiply connected surfaces. In *GMP*, pages 410–422, 2008.